Finite Element Eigenvalue Method for Solving Phase-Change Problems

Jiakang Zhong*
Zhejiang University, Hangzhou, People's Republic of China
Louis C. Chow†
University of Kentucky, Lexington, Kentucky 40506
and
Won Soon Chang‡
Wright Laboratory, Wright-Patterson Air Force Base, Ohio 45433

An eigenvalue method has been developed for solving multidimensional phase-change problems with the initial temperature at noncritical temperature. This method gives a closed-form analytical expression for the temperature field in terms of the eigenvalues and eigenfunctions of a characteristic equation derived from the generalized coordinate Lagrangian form of the heat conduction equation with phase change. The method yields reasonably accurate results with a coarse finite element mesh. It also has no critical time-step restrictions for stability. When long-time solutions are needed, excessive numerical computations are required by conventional finite difference or finite element methods due to the small time steps needed for time marching. With the present method, large time steps can be chosen to approximate the phase-change rate. In addition, only a few dominant eigenvalues and eigenfunctions are needed to achieve the same results obtained by using the complete set. These features result in very significant savings in computing time. For both the examples of one-dimensional solidification and solidification within a square, solutions can be obtained within a few iterations if appropriate relaxation factors are used. The results using the present method compare well with the exact solution for the one-dimensional problem and with a semianalytical similarity solution for the square.

Nomenclature

A = surface area
A_w, A'_w = defined by Eqs. (2c), (12d), and (18b)
$[A]$, a_{ij}, $a^{(e)}_{lm}$ = thermal stiffness matrix or tensor
a'_i, $a'^{(e)}_l$ = vector of nodal heat load resulting from specified nodal temperature
a''_i, $a''^{(e)}_l$ = vector of nodal heat load resulting from phase change
$\hat{a}''_i$, $\hat{a}''^{(e)}_l$ = defined by Eqs. (44) and (45), respectively
B_i = Biot number, $= hD/k_0$
$[B]$, b_{ij}, $b^{(e)}_{lm}$ = capacitance matrix or tensor
b_i, $b^{(e)}_l$ = vector of nodal heat load resulting from specified time derivative of nodal temperature
$[C]$, c_{ij}, $c^{(e)}_{lm}$ = boundary convection matrix or tensor
c = specific heat
c_i, $c^{(e)}_l$ = vector of boundary nodal heat load resulting from specified boundary nodal temperature
D = characteristic length
d'_s, d''_s, $\hat{d}''_s$ = defined by Eqs. (30), (31), and (43), respectively
E = defined by Eqs. (2a) and (12a)
E_f = defined by Eqs. (10a) and (12b)
E_w = defined by Eqs. (18a) and (20)
e_s = defined by Eq. (32)
F = local heat flux at second boundary condition
Fo = Fourier number, $= [k_0/\rho_0 c_0 D^2]t$
ΔFo = dimensionless time step
f = fraction of phase change, defined by Eq. (3a)
H = specific enthalpy
h = convection heat transfer coefficient
I = interface or area of interface
k = thermal conductivity
L = latent heat of fusion
n = outward normal to V
n_p = normal to interface toward a region
P = relaxation factor
p_s = principal coordinates, defined by Eq. (24)
p'_s = part of p_s, conduction effect
p''_s = part of p_s, phase-change effect
Q_i, Q'_i = defined by Eqs. (16) and (21)
q = generalized coordinates, defined by Eqs. (13) and (22)
$\dot{q}$ = dq/dt
R, R' = defined by Eqs. (2b), (10b), (12c), and (15)
Ste = Stefan number, $= c_0(T_f - T_0)/L$
T = temperature
t = time
V = volume
$W^{(e)}$ = phase-change effect, defined by Eq. (46)
$\dot{W}$ = time rate of phase-change effect, defined by Eq. (10a)
x_α = spatial coordinates
$[Y]$, y_{is} = eigenvector matrix, defined by Eq. (24)
α_s = defined by Eq. (26)
β_s = defined by Eq. (27)
Δ = triangular area
θ = dimensionless temperature, $= (T - T_0)/(T_f - T_0)$
λ_s = eigenvalues
π_s = defined by Eq. (29)
ρ = density
$c^{(s)}\,\phi^{(s)}_i$ = normalized eigenvectors

Presented as Paper 90-0544 at the AIAA 28th Aerospace Sciences Meeting, Reno, NV, Jan. 8–11, 1990; received Jan. 22, 1990; revision received July 11, 1990; accepted for publication July 21, 1990.

*Associate Professor, Mechanical Engineering Department.
†Professor, Mechanical Engineering Department. Member AIAA.
‡Research Scientist (WL/POOS), Aero Propulsion and Power Laboratory. Member AIAA.

Superscripts

(e)	=	finite element index
m	=	time level
(s)	=	eigenmode index

Subscripts

a	=	state before phase change
b	=	state after phase change
f	=	condition of fusion
g, h	=	condition at known node
i	=	generalized coordinate index
l	=	liquid state
l, m	=	condition at unknown node
o	=	initial, or arbitrary, reference condition
s	=	solid state, eigenmode index
w	=	wall
∞	=	ambient condition

Introduction

HEAT conduction with phase change occurs in nature and in many engineering systems, such as casting and welding of metals and alloys, freezing and thawing of water in lakes, as well as foodstuffs, thermal energy storage, and aerodynamic ablation, etc. Phase-change problems possess a high degree of nonlinearity since the phase-change interface is an unknown function of time. There are very few phase-change problems with exact solutions.[1] Several approximate and numerical techniques have been developed. The approximate methods, such as the integral method,[2] variational method[3] and perturbation method,[4,5] are usually restricted to one-dimensional problems. A semianalytical similarity solution[6] to the solidification of a liquid filling the quarter-space of a two-dimensional corner with constant-temperature boundary conditions is available. Many numerical methods have also been proposed, and a recent review of some of the finite-difference methods is given in Ref. 7. Other interesting methods are the thermal migration method,[8] fitting body coordinate system method,[9] thermal capacity or enthalpy method,[10,11] Green functions or boundary element method,[12,13] and finite element method using a moving mesh.[14] Many of these methods can deal only with some particular situations, and the applicability is limited. As a result of its inherent mathematical complexity, the multidimensional phase-change problem with an initial noncritical temperature has received very little attention in the published literature.[5,6]

Numerical solutions of phase-change problems usually can be divided into two types: temperature-based method or enthalpy-based method. In the former method, there is a difficulty associated with the discontinuity of the temperature gradient at the phase-change interface. To overcome this, calculations are made in two separate regions divided by the moving phase-change boundary. The latter method avoids the need to solve two moving boundary problems. The intent of this paper is to present an eigenvalue method with fixed finite elements using the enthalpy model. This method is based on the establishment of a enthalpy form of the generalized variational principle. The eigenvalue method provides a closed-form expression for the temperature field in terms of the eigenvalues and eigenfunctions of the problem. Closed-form expressions are highly desirable for coupled problems, such as the thermal-mechanical coupling in thermal stress calculations. Another advantage of the present method is the stability of the calculations to arbitrarily large time steps.

In this paper, first, we will consider the transient phase-change problem with constant thermophysical properties. Problems with variable properties will be considered in a forthcoming paper. To verify the validity of the eigenvalue method, calculations were performed for two phase-change problems. The first one is the one-dimensional solidification of a long slab, and the results are compared with the available exact solution.[1] The second problem is concerned with the solidification inside a square starting from one corner. Again, the results are compared with the semianalytical solution of solidification in an infinite two-dimensional corner.[6] In both examples, the initial temperatures are higher than the critical (or melting) temperature.

Generalized Variational Form for Phase-Change Heat Conduction

For an arbitrary volume V that is fixed in space (Fig. 1), the energy equation without convection transport is

$$\frac{\partial}{\partial x_\alpha}\left(k\frac{\partial\theta}{\partial x_\alpha}\right) = \rho\frac{\partial H}{\partial t} \tag{1}$$

The Galerkin variational formulation equivalent to Eq. (1) can be written as

$$\delta E + \delta R = \delta A_w \tag{2}$$

where

$$E = \frac{1}{2}\int_V k\left(\frac{\partial T}{\partial x_\alpha}\right)^2 \mathrm{d}V \tag{2a}$$

$$\delta R = \int_V \rho\frac{\partial H}{\partial t}\delta T\mathrm{d}V \tag{2b}$$

$$\delta A_w = \int_A k\frac{\partial T}{\partial n}\delta T\mathrm{d}A \tag{2c}$$

and A is the surface area of the control volume V.

The enthalpy within the control volume can be written as

$$H = fH_b + (1 - f)H_a \tag{3}$$

where the subscripts a and b represent the states of the substance in the control volume before and after phase change. For the case of solidification, a is the liquid state and b is the solid state, with $H_a = H_l = c_lT + L$, and $H_b = H_s = c_sT$, where L is the latent heat. For the case of melting, a and b denote the solid and liquid states, respectively, and $H_a = H_s = c_sT$, $H_b = H_l = c_lT + L$.

The mass fraction f is defined by

$$f = \frac{\rho_bV_b}{\rho_aV_a + \rho_bV_b} = \frac{V_b}{V_a + V_b} \tag{3a}$$

It can be shown that the variational form of Eq. (2) is the same as the one for the single-phase heat conduction[15] for the case of $f = 0$.

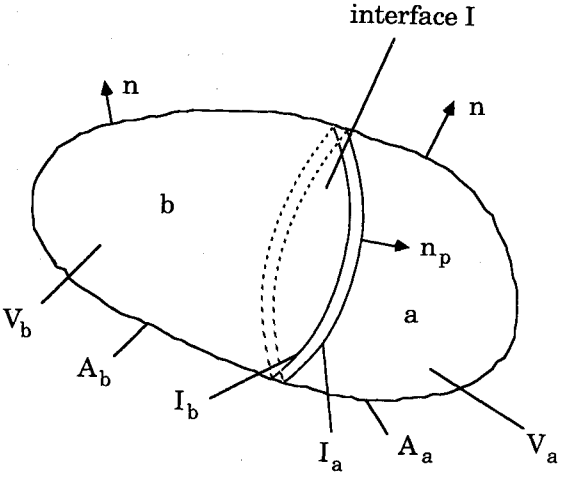

Fig. 1 System with phase change.

According to the variational form for a single phase,[15] we have in the a region:

$$\delta E_a + \delta R_a = (\delta A_w)_a \tag{4}$$

where

$$E_a = \frac{1}{2}\int_{V_a} k_a \left(\frac{\partial T}{\partial x_\alpha}\right)^2 \mathrm{d}V \tag{4a}$$

$$\delta R_a = \int_{V_a} \rho_a c_a \frac{\partial T}{\partial t}\,\delta T \mathrm{d}V \tag{4b}$$

$$(\delta A_w)_a = \int_{A_a + I_a} k_a \frac{\partial T}{\partial n}\,\delta T \mathrm{d}A$$

$$= \int_{A_a} k_a \frac{\partial T}{\partial n}\,\delta T \mathrm{d}A + \int_{I_a} k_a \frac{\partial T}{\partial n}\,\delta T \mathrm{d}A \tag{4c}$$

In the b region:

$$\delta E_b + \delta R_b = (\delta A_w)_b \tag{5}$$

where

$$E_b = \frac{1}{2}\int_{V_b} k_b \left(\frac{\partial T}{\partial x_\alpha}\right)^2 \mathrm{d}V \tag{5a}$$

$$\delta R_b = \int_{V_b} \rho_b c_b \frac{\partial T}{\partial t}\,\delta T \mathrm{d}V \tag{5b}$$

$$(\delta A_w)_b = \int_{A_b + I_b} k_b \frac{\partial T}{\partial n}\,\delta T \mathrm{d}A$$

$$= \int_{A_b} k_b \frac{\partial T}{\partial n}\,\delta T \mathrm{d}A + \int_{I_b} k_b \frac{\partial T}{\partial n}\,\delta T \mathrm{d}A \tag{5c}$$

Differentiating Eq. (3) with respect to time yields

$$\rho \frac{\partial H}{\partial t} = \mp \rho L \frac{\partial f}{\partial t} + f\rho c_b \frac{\partial T}{\partial t} + (1 - f)\,\rho c_a \frac{\partial T}{\partial t} \tag{6}$$

where the upper and lower signs correspond to the cases of solidification and melting, respectively. For constant properties, $H_l - H_s = L$ (this equality has been used earlier).

Substituting Eq. (6) into Eq. (2b),

$$\partial R = \mp \int_V \rho L \frac{\partial f}{\partial t}\,\delta T \mathrm{d}V + \delta R_a + \delta R_b \tag{7}$$

Substituting Eq. (7) into Eq. (2) and using Eqs. (4), (4c), (5), (5c), and

$$\delta E = \delta E_a + \delta E_b$$

and

$$\delta A_w = \int_{A_a + A_b} k_{a,b} \frac{\partial T}{\partial n}\,\delta T \mathrm{d}A$$

we obtain

$$\int_{I_a} k_a \frac{\partial T}{\partial n}\,\delta T \mathrm{d}A + \int_{I_b} k_b \frac{\partial T}{\partial n}\,\delta T \mathrm{d}A = \pm \int_V \rho L \frac{\partial f}{\partial t}\,\delta T \mathrm{d}V \tag{8}$$

If we denote n_p as the normal to interface I toward the a region and notice that δT is arbitrary, Eq. (8) can be written as

$$\int_{I_b} k_b \frac{\partial T}{\partial n_p}\,\mathrm{d}A - \int_{I_a} k_a \frac{\partial T}{\partial n_p}\,\mathrm{d}A = \pm \int_V \rho L \frac{\partial f}{\partial t}\,\mathrm{d}V \tag{9}$$

This is the energy conservation relation of the phase change across the interface. So far, it has been shown that the generalized variational principle [Eq. (2)] is applicable whether or not the phase change exists in the system.

If we substitute Eq. (6) into Eq. (2), the variational principle is converted to the following form, with temperature being the dependent variable instead of enthalpy:

$$\delta E + \delta E_f + \delta R' = \delta A_w \tag{10}$$

where

$$E_f = -\int_V \dot{W} T \mathrm{d}V, \qquad \dot{W} = \pm \rho L \frac{\partial f}{\partial t} \tag{10a}$$

$$\delta R' = \int_V \rho c \frac{\partial T}{\partial t}\,\delta T \mathrm{d}V \tag{10b}$$

Dimensionless Variational Form and Corresponding Lagrangian Equation

The variational principle can be expressed in nondimensional form by introducing the following nondimensional quantities:

$$\bar{x}_\alpha = \frac{x_\alpha}{D}, \qquad \bar{A} = \frac{A}{D^2}, \qquad \bar{V} = \frac{V}{D^3}$$

$$\bar{k} = \frac{k}{k_0}, \qquad \bar{\rho} = \frac{\rho}{\rho_0}, \qquad \bar{c} = \frac{c}{c_0}$$

$$\theta = \frac{T - T_0}{T_f - T_0}, \qquad Fo = \frac{k_0}{\rho_0 c_0 D^2} t, \qquad B_i = \frac{hD}{k_0}$$

$$Ste = \frac{c_0(T_f - T_0)}{L}, \qquad \bar{F} = \frac{DF}{k_0(T_f - T_0)}$$

$$\bar{\dot{W}} = \frac{D^2}{k_0(T_f - T_0)}, \qquad \dot{W} = \pm \bar{\rho} \frac{\partial f}{\partial Fo}(Ste)^{-1} \tag{11}$$

The nondimensional variation form of Eq. (10) is

$$\delta E + \delta E_f + \delta R' = \delta A_w \tag{12}$$

where

$$E = \frac{1}{2}\int_V k \left(\frac{\partial \theta}{\partial x_\alpha}\right)^2 \mathrm{d}V \tag{12a}$$

$$E_f = -\int_V \dot{W}\theta \mathrm{d}V \tag{12b}$$

$$\delta R' = \int_V \rho c \frac{\partial \theta}{\partial Fo}\,\delta\theta \mathrm{d}V \tag{12c}$$

$$\delta A_w = \int_A k \frac{\partial \theta}{\partial n}\,\delta\theta \mathrm{d}A \tag{12d}$$

The bars over the dimensionless variables have been omitted in the preceding equations.

Now, the temperature field is expressed by using a set of generalized coordinates $q_i(Fo)$:

$$\theta = \theta(q_i, x_\alpha), \qquad i = 1,2, \ldots, n \tag{13}$$

From the variational principle [Eq. (12)], the following Lagrangian equation can be derived:

$$\frac{\partial(E + E_f)}{\partial q_i} + \frac{\partial R'}{\partial \dot{q}_i} = Q_i, \qquad i = 1, 2, \ldots, n \tag{14}$$

where

$$R' = \int_V \frac{1}{2} \rho c \left(\frac{\partial \theta}{\partial Fo}\right)^2 \mathrm{d}V \tag{15}$$

$$Q_i = \int_A k \frac{\partial \theta}{\partial n} \frac{\partial \theta}{\partial q_i} \mathrm{d}A \tag{16}$$

The variational principle [Eq. (12)] and corresponding Lagrangian equation [Eq. (14)] are applicable to any boundary conditions. We will consider the following nondimensional boundary conditions:

$$\theta = \theta_w \qquad \text{on } A_1 \tag{17a}$$

$$k \frac{\partial \theta}{\partial n} = F \qquad \text{on } A_2 \tag{17b}$$

$$k \frac{\partial \theta}{\partial n} = B_i(\theta_\infty - \theta) \qquad \text{on } A_3 \tag{17c}$$

where A_1, A_2, and A_3 are the surface areas for boundary conditions of the first, second, and third kinds, respectively. Equation (12) can be written as

$$\delta E + \delta E_w + \delta E_f + \delta R' = \delta A'_w \tag{18}$$

where

$$\delta E_w = \int_{A_3} B_i \theta \delta\theta \mathrm{d}A \tag{18a}$$

$$\delta A'_w = \int_{A_2, A_3} (F + B_i \theta_\infty) \delta\theta \mathrm{d}A \tag{18b}$$

This variational form [Eq. (18)] leads to the following Lagrangian equation:

$$\frac{\partial(E + E_w + E_f)}{\partial q_i} + \frac{\partial R'}{\partial \dot{q}_i} = Q'_i \tag{19}$$

where

$$E_w = \int_{A_3} \frac{1}{2} B_i \theta^2 \mathrm{d}A \tag{20}$$

$$Q'_i = \int_{A_2, A_3} (F + B_i \theta_\infty) \frac{\partial \theta}{\partial q_i} \mathrm{d}A \tag{21}$$

Discrete Analytical Solution

Suppose that the finite element approximation function for θ is chosen as

$$\theta^{(e)} = N_g^{(e)} \theta_g^{(e)} + N_l^{(e)} q_l^{(e)} \tag{22}$$

where $N_l^{(e)}(x_a)$ is the local position function, and $q_l^{(e)}$ and $\theta_g^{(e)}$ represent the unknown value of θ at node l and the known value at node g, respectively. Following a procedure similar to Ref. 15 together with Eq. (22), the global form of functions E, E_f, R', E_w, and Q'_i can be evaluated by summing the contribution of the individual elements from Eqs. (12a), (12b), (15), (20), and (21). Equation (19) can be cast into the following ordinary differential equation system:

$$[A + C]\{q\} + [B]\{\dot{q}\} = \{Q' - a' - a'' - b - c\} \tag{23}$$

where $[A] = (a_{ij})_{n\times n}$, $[B] = (b_{ij})_{n\times n}$, and $[C] = (c_{ij})_{n\times n}$ are the symmetric matrices, with n the number of generalized coordinates. $\{Q'\}$, $\{a'\}$, $\{a''\}$, $\{b\}$, and $\{c\}$ are the n-dimensional vectors. The expressions for $a_{lm}^{(e)}$, $b_{lm}^{(e)}$, $c_{lm}^{(e)}$, $a_l'^{(e)}$, $a_l''^{(e)}$, $b_l^{(e)}$, $c_l^{(e)}$, and $Q_l^{(e)}$, for an element are given in Appendix A.

Equation (23) can be converted to an eigenvalue problem, and the discrete analytical solution can be obtained by following a similar procedure given in Ref. 15. We introduce the principal coordinates p_s ($s = 1, \ldots, n$), which is defined by

$$\{q\} = [Y]\{p\} \tag{24}$$

where $[Y] = (y_{is})_{n\times n}$ and $y_{is} = c^{(s)}\phi_i^{(s)}$, which are the normalized eigenvectors given later in the paper.

The equation for the principal coordinates can be deduced from Eq. (23) as

$$\alpha_s p_s + \beta_s \dot{p}_s = \pi_s - d'_s - d''_s - e_s \tag{25}$$

where

$$\alpha_s = \{c^{(s)}\phi^{(s)}\}^T [A + C]\{c^{(s)}\phi^{(s)}\} \tag{26}$$

$$\beta_s = \{c^{(s)}\phi^{(s)}\}^T [B]\{c^{(s)}\phi^{(s)}\} \tag{27}$$

$$\alpha_s = \lambda_s \beta_s \tag{28}$$

$$\pi_s = \sum_{i=1}^{n} Q'_i c^{(s)}\phi_i^{(s)} \tag{29}$$

$$d'_s = \sum_{i=1}^{n} (a'_i + c_i) c^{(s)}\phi_i^{(s)} \tag{30}$$

$$d''_s = \sum_{i=1}^{n} a''_i c^{(s)}\phi_i^{(s)} \tag{31}$$

$$e_s = \sum_{i=1}^{n} b_i c^{(s)}\phi_i^{(s)} \tag{32}$$

λ_s and $c^{(s)}\phi_i^{(s)}$ are the eigenvalues and the corresponding normalized eigenvectors determined from the following eigenequation:

$$[A + C - \lambda B]\{\phi\} = \{0\} \tag{33}$$

The numerical calculations for Eq. (33) can be carried out using EISPACK[16] or IBM library routines.

Equation (25) can be separated into

$$p_s = p'_s + p''_s \tag{34}$$

$$\alpha_s p'_s + \beta_s \dot{p}'_s = \pi_s - d'_s - e_s \tag{35}$$

$$\alpha_s p''_s + \beta_s \dot{p}''_s = -d''_s \tag{36}$$

In Eq. (34), p'_s is the contribution to p_s due to pure conduction alone,[15] and p''_s indicates the part due to phase change.

For $\lambda_s \to \infty$, we can set $\alpha_s = 1$ to normalize the eigenvector, and the solutions for Eqs. (35) and (36) are

$$p'_s(Fo) = \pi_s - d'_s - e_s \tag{37}$$

$$p''_s = -d''_s \tag{38}$$

For $\lambda_s \neq \infty$, by setting $\beta_s = 1$ for normalization, the solutions to Eqs. (35) and (36) are

$$p_s'(Fo) = \exp[-\lambda_s(Fo - Fo_0)] \left\{ \int_{Fo_0}^{Fo} (\pi_s - d_s' - e_s) \exp[\lambda_s(Fo - Fo_0)]\, dFo + p_s(Fo_0) \right\} \quad (39)$$

and

$$p_s''(Fo) = \exp[-\lambda_s(Fo - Fo_0)] \left\{ \int_{Fo_0}^{Fo} (-d_s'') \exp[\lambda_s(Fo - Fo_0)]\, dFo \right\} \quad (40)$$

where $p_s(Fo_0)$ is the initial value of p_s and can be evaluated from the initial temperature distribution.

If $(\pi_s - d_s' - e_s)$ is independent of time, Eq. (39) can be integrated to yield:

For $\lambda_s \neq 0$:

$$p_s'(Fo) = \frac{\pi_s - d_s' - e_s}{\lambda_s} \left\{ 1 - \exp[-\lambda_s(Fo - Fo_0)] \right\} + p_s(Fo_0) \exp[-\lambda_s(Fo - Fo_0)] \quad (41a)$$

For $\lambda_s = 0$:

$$p_s'(Fo) = (\pi_s - d_s' - e_s)(Fo - Fo_0) + p_s(Fo_0) \quad (41b)$$

The integration of Eq. (40) needs special discussion. The variable d_s'' represents a total phase-change aspect of the system. Using Eq. (31), the expression for $a_l''^{(e)}$ in Appendix A, and the nondimensional form of $\dot{W}$ in Eq. (11), d_s'' can be written as

$$d_s'' = \frac{\partial \hat{d}_s''}{\partial Fo} \quad (42)$$

where

$$\hat{d}_s'' = \sum_{i=1}^{n} \hat{a}_s''\, c^{(s)} \phi_i^{(s)} \quad (43)$$

$$\hat{a}_i'' = \sum_{l} \hat{a}_l''^{(e)} \Delta_{li}^{(e)} \quad (44)$$

$$\hat{a}_l''^{(e)} = -\int_{V^{(e)}} W^{(e)} N_l^{(e)} dV \quad (45)$$

$$W^{(e)} = \pm \rho^{(e)} (Ste)^{-1} f^{(e)} \quad (46)$$

In Eq. (44), $\Delta_{li}^{(e)} = 1$ for $l = i$ and 0 for $l \neq i$.

The nonlinearity of the phase-change problem is reflected in the unknown f or $\hat{d}_s''$. The time domain is divided into several stages, and over each stage $\hat{d}_s''$ is approximated as a linear function of time. Thus, the time derivative in Eq. (42) can be written as a backward difference,

$$d_s'' = \frac{(\hat{d}_s'')_m - (\hat{d}_s'')_{m-1}}{\Delta Fo} \quad (47)$$

and d_s'' is constant in the time increment $\Delta Fo = (Fo)_m - (Fo)_{m-1}$. Equation (40) can be integrated to give

For $\lambda \neq 0$:

$$p_s''(Fo) = \frac{-d_s''}{\lambda_s} \{1 - \exp[-\lambda_s(Fo - Fo_0)]\} \quad (48a)$$

For $\lambda = 0$:

$$p_s''(Fo) = -d_s''(Fo - Fo_0) \quad (48b)$$

Here, Fo and Fo_0 represent $(Fo)_m$ and $(Fo)_{m-1}$, respectively.

From the preceding equations, the unknowns p_s', p_s'', p_s, q_i, and $f^{(e)}$ (or $\hat{d}_s''$) at time level m can be obtained by an iterative process provided that these are known at the previous time level $m - 1$. The initial values $p_s(Fo_0)$ in Eqs. (41) can be evaluated from the known temperature distribution $q_i(Fo_0)$ using the following (see Ref. 15):

$$\{p\} = [Y]^T [B] \{q\}, \qquad \lambda_s \neq \infty$$
$$= [Y]^T [A + C] \{q\}, \qquad \lambda_s \to \infty \quad (49)$$

Description of Two-Phase Triangular Elements

We consider the triangular element with three nodes (I, J, K). The temperatures at these nodes are either a function of time or specified as boundary conditions. The phase-change interface divides the element into a and b portions. The definition of fraction $f^{(e)}$ in an element is given by Eq. (3a) and $f^{(e)}$ varies from 0 (no phase change) to 1 (complete phase change). Figure 2 shows all of the possible cases of a two-phase element. The fraction $f^{(e)}$ is determined by using linear interpolation of nodal temperatures.

In the numerical procedure, the first step would be to take $f_m^{(e)} = f_{m-1}^{(e)}$, and the system of equations may be solved for the unknown temperature field at time level m provided the solution is known at time level $m - 1$. This allows a new $f_m^{(e)}$ to be calculated. An improved solution can then be found by solving again for the unknown temperature field using the updated values of the fraction $f^{(e)}$. This process is repeated until the convergence requirement is satisfied.

Numerical Examples

To test the validity of the numerical procedure, we use two-dimensional triangular elements to solve a one-dimensional half-space solidification problem with $k_s = k_l = \rho_s c_s = \rho_l c_l = 1$. The initial temperature is uniform with $\theta_0 = 1.3$, which is greater than the fusion temperature $\theta_f = 1$. For $Fo > 0$, the surface temperature θ_w at $x = 0$ is maintained at zero. The computational domain for the semi-infinite half-space is shown in Fig. 3. Adiabatic boundary conditions are imposed on the surfaces at $x = 5.5$, $y = 0$, and $y = 0.2$. The results of the interface position vs time and the temperature distribution along the midline ($y = 0.1$) for $Ste = 4$ are shown in Table 1 and Fig. 4, respectively. Also shown are the results from the exact solution given in Ref. 1. The relaxation factor P used is 1. Only eight or nine iterations are needed to achieve a convergence criterion so that the percentage change between the temperatures or two successive iterations at every node is less than 0.005. It can be seen that the present results agree very well with the exact solution.

For $Ste = 0.25$, the results of the interface positions and temperature distributions are presented in Table 2 and Fig. 5, respectively. For this small Ste, underrelaxation was used with $P = 0.1$. The number of iterations is usually less than 30. Again, the agreement between the present results and the exact solution is very good.

It should be noted here that there is no time-step restriction for the present numerical technique as far as numerical stability is concerned. The results shown in Figs. 4 and 5 at any Fo were obtained directly from the initial condition. The effects of time-step size on the accuracy of the results will be discussed subsequently.

The second example considered is the two-dimensional solidification within a square at an initial temperature $\theta_0 = 1.3$. At $Fo > 0$, the surfaces at $x = 0$ and $y = 0$ are maintained at $\theta_w = 0$, and the surfaces at $x = 1$ and $y = 1$ are adiabatic. As a result of symmetry, the finite element arrangement is shown for only half of the square (see Fig. 6). For $Ste = 4$,

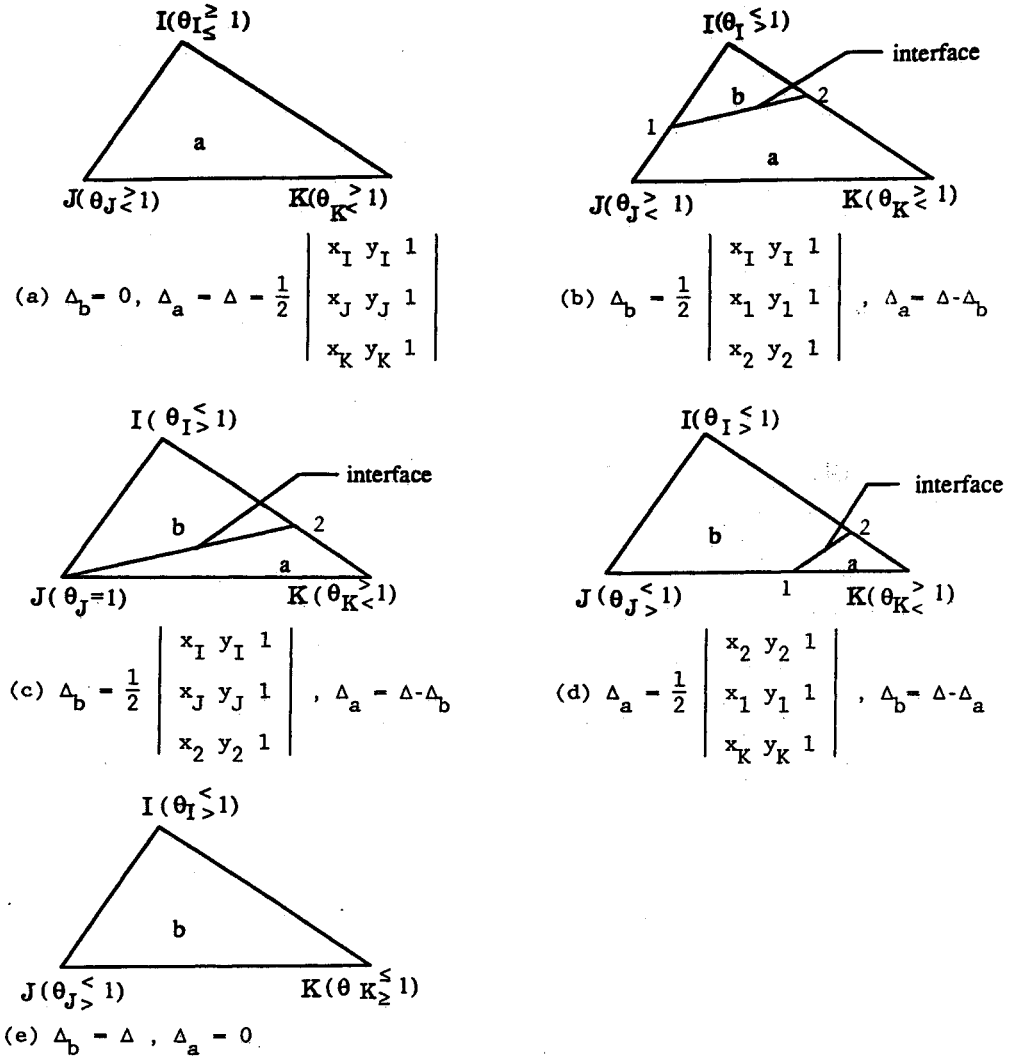

Fig. 2 Two-phase triangular elements ($\theta \gtrless 1$, etc.: upper sign for freezing; lower sign for melting).

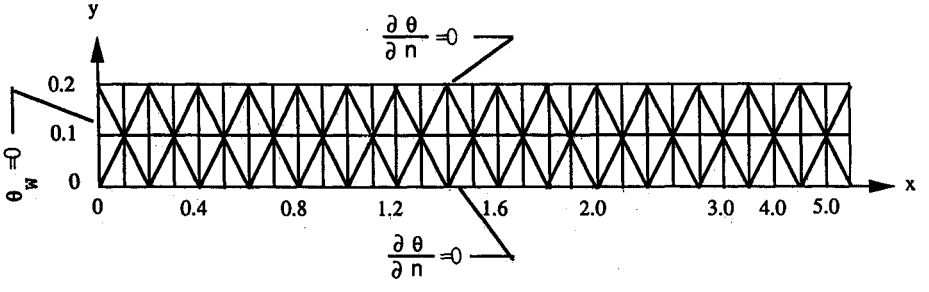

Fig. 3 Finite elements for one-dimensional half-space.

Table 1 Comparison of interface positions for solidification in one-dimensional half-space (Ste = 4)

		Present method, ΔFo =				
Fo	Exact	0.05	0.1	0.2	0.5	Fo – 0
0.1	0.448	0.463	0.468			0.468
0.2	0.633	0.645	0.648	0.658		0.658
0.3	0.775	0.785	0.787			0.803
0.4	0.895	0.893	0.897	0.908		0.927
0.5	1.001	0.993	1.000		1.036	1.036
0.6	1.096	1.087	1.092	1.102		1.133
0.7	1.184	1.174	1.180			1.224
0.8	1.266	1.252	1.260	1.270		1.306
0.9	1.343	1.325	1.329			1.386
1.0	1.415	1.394	1.398	1.409	1.438	1.461

the temperature distributions along the symmetry line ($x = y$) and the interface positions are various Fo are given in Figs. 7 and 8, respectively. The time step chosen was 0.01. Also plotted in Figs. 7 and 8 are the analytical results of freezing in an infinite two-dimensional corner.[6] The present results agree quite well with the analytical solution for the temperature field, including the symmetry line ($x = y$) even though the analytical solution is for the infinite quarter-space instead of a square. However, the interface positions obtained by the present method disagree somewhat with the analytical results. The main reason for the slight disagreement is because the interface positions are obtained by a simple linear interpolation of the nodal temperatures (see Fig. 2). In addition, the disagreement is larger near the symmetry line because the length of the grid in the 45-deg direction is larger than that in the horizontal direction.

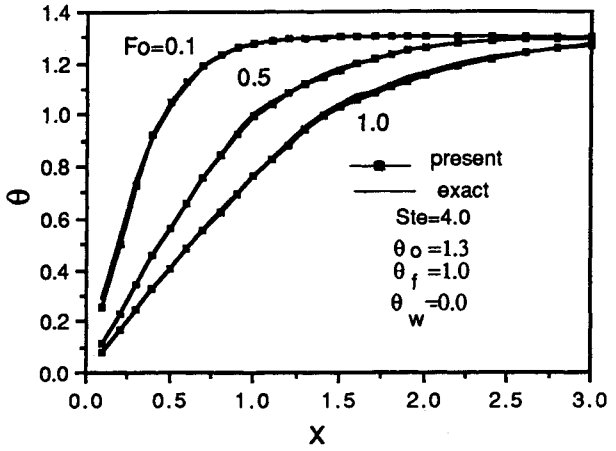

Fig. 4 Temperature distributions during freezing of one-dimensional half-space (*Ste* = 4).

Table 2 Comparison of interface positions for solidification in one-dimensional half-space (*Ste* = 0.25)

		Present method, ΔFo =		
Fo	Exact	0.1	0.5	*Fo*
0.1	0.199	0.200		0.200
0.2	0.281	0.287		
0.3	0.344	0.353		0.356
0.4	0.397	0.408		
0.5	0.444	0.455	0.458	
0.6	0.487	0.500		
0.7	0.526	0.538		0.540
0.8	0.562	0.574		
0.9	0.596	0.610		
1.0	0.628	0.641	0.647	0.647

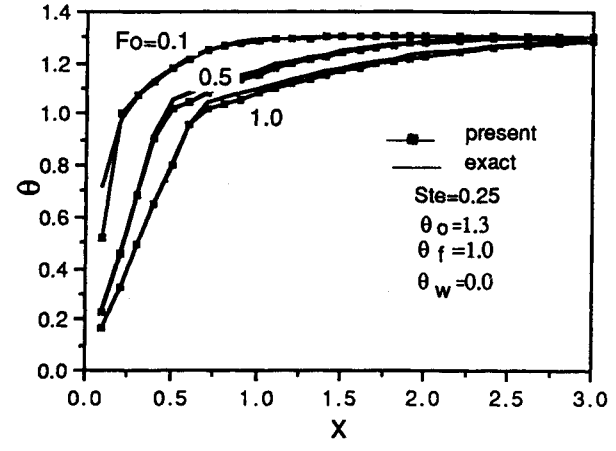

Fig. 5 Temperature distributions during freezing of one-dimensional half-space (*Ste* = 0.25).

As in the previous example, with *Ste* = 4, no underrelaxation (P = 1) was needed to achieve convergence. However, when the Stefan number is small, phase-change effects assert a more dominant role in the heat transfer process and the problem becomes more nonlinear. In such cases, underrelaxation is required to obtain convergence. Figure 9 shows the effect of the relaxation parameter P on the iteration process for the temperature at a location inside the square (x = 0.1 and y = 0.05) at *Fo* = 0.1. The Stefan number is 0.1. For P = 0.5 and 1, the iterative process does not converge. The process converges only if P is 0.4 or less. The convergence is fastest with P = 0.3. Finally, based on the observations from a large number of computer runs, it can be concluded that the iterative process depends predominately on *Ste* and very little on *Fo* and the time-step size.

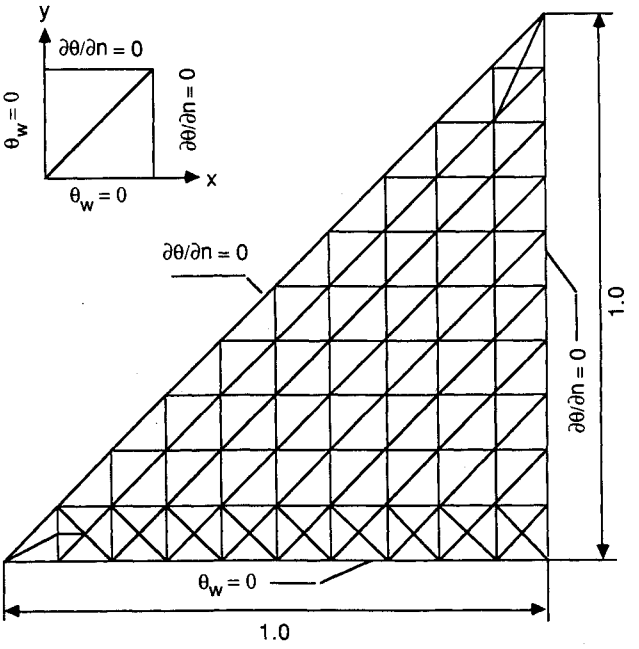

Fig. 6 Finite elements for a two-dimensional square.

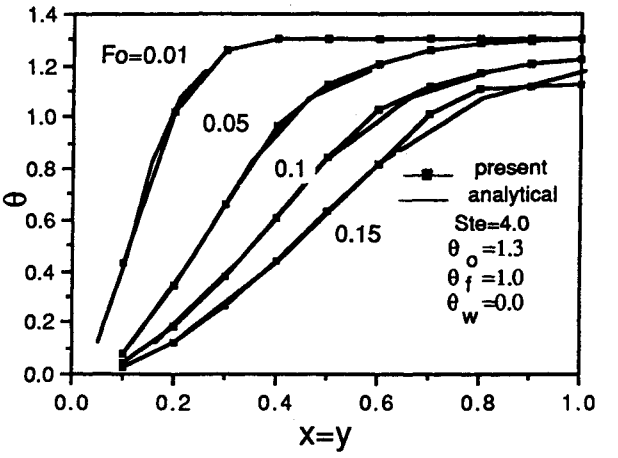

Fig. 7 Temperature distribution along symmetry line.

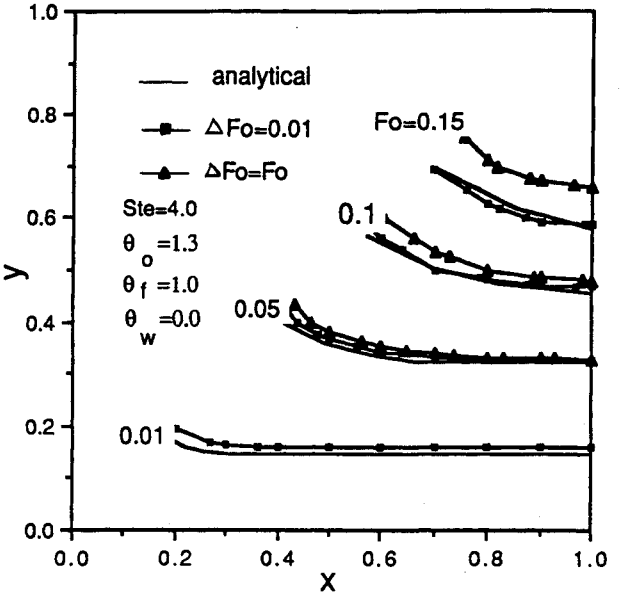

Fig. 8 Interface positions vs time.

Table 3 Contributions of eigenmodes for solidification in one-dimensional half-space ($Fo = 0.5$)

		$Ste = 4$			$Ste = 0.25$		
s	λ_s	p_s'	p_s''	p_s	p_s'	p_s''	p_s
1	0.0788	1.1877	0.0021	1.1898	1.2051	0.0066	1.2117
2	0.7360	0.3027	0.0055	0.3082	0.3462	0.0187	0.3649
3	2.0816	0.1063	0.0069	0.1132	0.1577	0.0285	0.1862
4	4.1478	−0.0348	−0.0058	−0.0406	−0.0778	−0.0339	−0.1117
5	7.0166	0.0101	0.0030	0.0131	0.0402	0.0362	0.0764
6	10.826	0.0020	−0.0003	0.0017	0.0189	0.0325	0.0514
7	15.352	0.0000	0.0025	0.0025	−0.0090	−0.0280	−0.0370
8	21.408	−0.0003	−0.0033	−0.0036	0.0035	0.0208	0.0243
9	27.806	0.0002	0.0023	0.0025	−0.0012	−0.0126	−0.0138
10	35.200	0.0001	0.0012	0.0013	−0.0005	−0.0083	−0.0088
11	44.014	−0.0000	0.0001	0.0001	0.0001	0.0018	0.0019
12	49.058	0.0000	−0.0007	−0.0007	−0.0000	−0.0009	−0.0009
13	63.771		−0.0014	−0.0014		0.0034	0.0034
14	82.478		−0.0008	−0.0008		0.0059	0.0059
15	105.89		−0.0002	−0.0002		−0.0062	−0.0062
16	131.47		0.0006	0.0006		−0.0049	−0.0049
17	160.11		0.0004	0.0004		0.0034	0.0034
18	196.85		−0.0001	−0.0001		0.0014	0.0014
19	232.80		−0.0003	−0.0003		−0.0001	−0.0001
20	265.69		−0.0003	−0.0003		−0.0000	−0.0000

Table 4 Contributions of eigenmodes for solidification in a square ($Fo = 0.1$)

s	λ_s	p_s'	p_s''	p_s
1	4.9407	−0.5045	−0.0067	−0.5112
2	25.304	0.0507	0.0030	0.0537
3	46.373	0.0014	0.0022	0.0036
4	67.625	−0.0021	−0.0042	−0.0063
5	92.987	−0.0006	0.0002	−0.0004
6	135.99	0.0008	0.0011	0.0019
7	137.37	−0.0006	−0.0015	−0.0021
8	164.80	−0.0004	−0.0021	−0.0025
9	225.02	0.0000	0.0006	0.0006
10	236.05	0.0001	0.0012	0.0013
11	269.80	0.0000	−0.0003	−0.0003
12	285.75		−0.0001	−0.0001
13	344.78		0.0004	0.0004
14	373.79		−0.0007	−0.0007
15	412.80		−0.0008	−0.0008

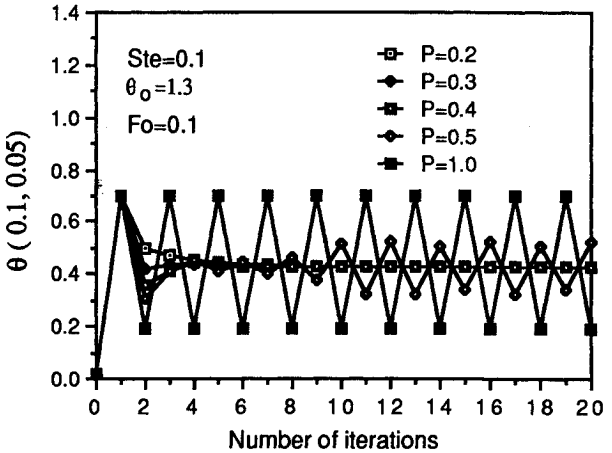

Fig. 9 Effect of relaxation factor P on iterative process.

Effects of Time Step on Accuracy

One of the major advantages of the eigenvalue method for the heat conduction problem without phase change is that the numerical solution contains no error in the time domain and there is no time-step restriction due to numerical stability consideration.[15] Hence, the time step ΔFo should be as large as possible. However, with phase change, in the integration of Eq. (40), a backward difference approximation to d_s'' in Eq. (42) was used. Fortunately, the variable d_s'', which is an indication of the fraction of the domain that has undergone phase change, is usually a slowly varying function of Fo. This allows rather large time steps to be taken and still retains good accuracy of the numerical solution. For the unidimensional solidification problem, the influence of ΔFo on the numerical accuracy is shown in Tables 1 and 2. Although the results are better for smaller ΔFo, the results using the largest possible δFo ($= Fo$) are still reasonably accurate. The temperature distributions obtained using $\Delta Fo = Fo$ compare very well with the exact solution (see Figs. 4 and 5).

For the case of two-dimensional solidification within a square, the results obtained with $\Delta Fo = 0.01$ and Fo are compared with the analytical solution of freezing at the corner of the infinite quarter-space in Fig. 7. It is clear that the size of the time step has very little influence on the accuracy of the numerical results, except near the point of complete freezing.

If a quadratic approximation for $\hat{d}_s''$ is used instead of a linear approximation, even larger time steps can be taken without sacrificing the accuracy of the numerical solution.

Partial Set of Eigenvalues and Eigenvectors

For the case of heat conduction with no phase change, an important feature of the eigenvalue method is that only the dominant (small) eigenvalues and their corresponding eigenvectors need to be calculated to achieve accurate results.[15] This characteristic also exists when phase change occurs. Tables 3 and 4 indicate the contribution of the dominant eigenmodes and their contribution to the principal coordinates p_s', p_s'', and p_s for the one- and two-dimensional problems. It is safe to state that the eigenmodes with $\lambda_s > 200$ do not contribute to the principal coordinates and, in turn, to the generalized coordinates (nodal temperatures). Temperatures at some representative locations for both examples are also plotted as a function of the number of eigenmodes in Figs. 10 and 11. Again, it is clear that only a small fraction of the eigenmodes are needed, namely, those with smaller eigenvalues. Since most of the computer time is used to compute the eigenvalues and eigenvectors, exploitation of this feature clearly leads to significant savings in computer time.

Conclusions

The finite element eigenvalue method presented herein can deal with the multidimensional heat conduction problem with phase change initially not at the critical temperature. The

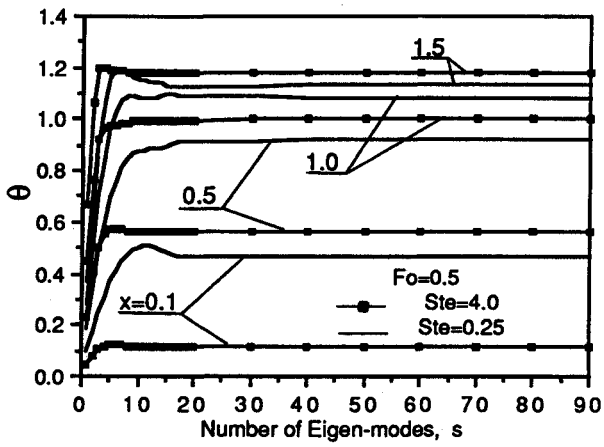

Fig. 10 Contribution of eigenmodes for freezing in a one-dimensional half-space.

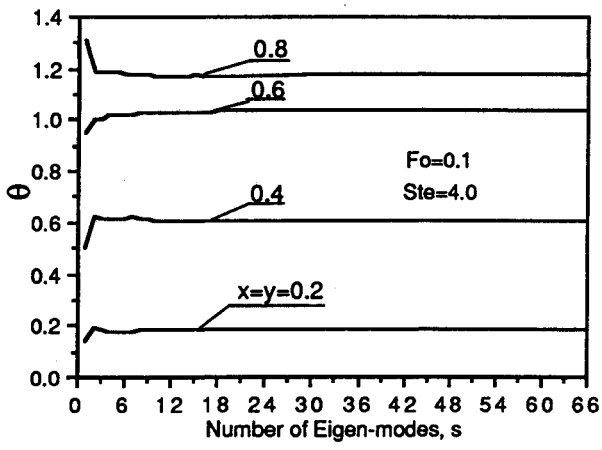

Fig. 11 Contribution of eigenmodes for freezing in a square.

present method is attractive because of its inherent stability, rapid convergence, and use of a relatively coarse element mesh and arbitrarily large time steps. The use of large time step leads to very significant savings in computer time when solutions with long time duration are needed. With conventional methods, time marching with very small time steps is necessary. The characteristic that accurate results can be obtained only with the dominant eigenmodes can lead to further reduction in computer time. Furthermore, this method provides closed-form expressions for the temperature field. These closed-form expressions are very convenient for solving coupled problems, such as solid-fluid and thermal-structure interactions.

Appendix A

By using the element shape function [Eq. (22)] in Eqs. (12a), (12b), (15), (20), and (21), the functions $E^{(e)}$, $E_f^{(e)}$, $R'^{(e)}$, $E_w^{(e)}$, and $Q_i'^{(e)}$ for an element can be evaluated as follows:

$$E^{(e)} + E_f^{(e)} = \frac{1}{2} a_{lm}^{(e)} q_l^{(e)} q_m^{(e)} + (a_l'^{(e)} + a_l''^{(e)}) q_l^{(e)} + a_o'^{(e)} + a_o''^{(e)} \tag{A1}$$

where

$$a_{lm}^{(e)} = a_{ml}^{(e)} = \int_{V^{(e)}} k \frac{\partial N_l^{(e)}}{\partial x_\alpha} \frac{\partial N_m^{(e)}}{\partial x_\alpha} \, dV$$

$$a_l'^{(e)} = \left(\int_{V^{(e)}} k \frac{\partial N_g^{(e)}}{\partial x_\alpha} \frac{\partial N_l^{(e)}}{\partial x_\alpha} \, dV \right) \theta_g^{(e)}$$

$$a_l''^{(e)} = - \int_{V^{(e)}} \dot{W}^{(e)} N_l^{(e)} \, dV$$

$$a_o'^{(e)} = \frac{1}{2} \left(\int_{V^{(e)}} k \frac{\partial N_g^{(e)}}{\partial x_\alpha} \frac{\partial N_h^{(e)}}{\partial x_\alpha} \, dV \right) \theta_g^{(e)} \theta_h^{(e)}$$

$$a_o'' = \left(- \int_{V^{(e)}} \dot{W}^{(e)} N_g^{(e)} dV \right) \theta_g^{(e)}$$

$$R'^{(e)} = \frac{1}{2} b_{lm}^{(e)} \dot{q}_l^{(e)} \dot{q}_m^{(e)} + b_l^{(e)} \dot{q}_l^{(e)} + b_o^{(e)} \tag{A2}$$

where

$$b_{lm}^{(e)} = b_{ml}^{(e)} = \int_{V^{(e)}} \rho c N_l^{(e)} N_m^{(e)} dV$$

$$b_l^{(e)} = \left(\int_{V^{(e)}} \rho c N_g^{(e)} N_l^{(e)} dV \right) \dot{\theta}_g^{(e)}$$

$$b_o = \frac{1}{2} \left(\int_{V^{(e)}} \rho c N_g^{(e)} N_h^{(e)} dV \right) \dot{\theta}_g^{(e)} \dot{\theta}_h^{(e)}$$

$$E_w^{(e)} = \frac{1}{2} c_{lm}^{(e)} q_l^{(e)} q_m^{(e)} + c_l^{(e)} q_l^{(e)} + c_o^{(e)} \tag{A3}$$

where

$$c_{lm}^{(e)} = c_{ml}^{(e)} = \int_{A_3^{(e)}} B_l^{(e)} N_l^{(e)} N_m^{(e)} dA$$

$$c_l^{(e)} = \left(\int_{A_3^{(e)}} B_l^{(e)} N_g^{(e)} N_l^{(e)} dA \right) \theta_g$$

$$c_o^{(e)} = \frac{1}{2} \left(\int_{A_3^{(e)}} B_l^{(e)} N_g^{(e)} N_h^{(e)} dA \right) \theta_g^{(e)} \theta_h^{(e)}$$

and

$$Q_l'^{(e)} = \int_{A_2^{(e)}, A_3^{(e)}} (F^{(e)} + B_l^{(e)} \theta_\infty^{(e)}) N_l^{(e)} dA \tag{A4}$$

The global functions E, E_f, R', E_w, and Q_i can be obtained by summing the contributions from the individual elements. Substituting the resulting global functions into Eq. (19) results in the ordinary differential equation system [Eq. (23)]. The matrices $[A]$, $[B]$, $[C]$, $\{a'\}$, $\{a''\}$, $\{b\}$, $\{c\}$, and $\{Q'\}$ can also be obtained by direct assembly over all elements.

Acknowledgments

This work is supported by the Wright Research and Development Center under Contract F33615-87-C-2777. Micheal Morgan is the contract monitor.

References

[1]Carslaw, H. S., and Jaeger, J. C., *Conduction of Heat in Solids*, Oxford Univ. Press, London, England, 1959.

[2]Goodman, T. R., "Application of Integral Methods to Transient Non-Linear Heat Transfer," *Advances in Heat Transfer*, Vol. 1, 1964, pp. 55–122.

[3]Biot, M. A., *Variational Principles in Heat Transfer, A Unified Lagrangian Analysis of Dissipative Phenomena*, Clarendon, Oxford, England, 1970.

[4]Weinbaum, S., and Jiji, L. M., "Singular Perturbation Theory for

Melting or Freezing in Finite Domains Initially Not at the Fusion Temperature," *Journal of Applied Mechanics*, Vol. 44, No. 1, 1977, pp. 25–30.

[5]Gutman, L. N., "On the Problem of Heat Transfer in a Phase-Change Slab Initially Not at the Critical Temperature," *Journal of Heat Transfer*, Vol. 109, No. 1, 1987, pp. 5–9.

[6]Rathjen, K. A., and Jiji, L. M., "Heat Conduction with Melting or Freezing in a Corner," *Journal of Heat Transfer*, Vol. 93, No. 1, 1971, pp. 101–109.

[7]Pham, Q. T., "A Note on Some Finite-Difference Methods for Heat Conduction with Phase Change," *Numerical Heat Transfer*, Vol. 11, No. 3, 1987, pp. 353–359.

[8]Crank, J., and Gupta, R. S., "Isotherm Migration Method in Two Dimensions," *International Journal of Heat and Mass Transfer*, Vol. 18, No. 9, 1975, pp. 1101–1107.

[9]Duda, J. L., Malone, M. F., and Notter, R. H., "Analysis of Two-Dimensional Diffusion-Controlled Moving Boundary Problems," *International Journal of Heat and Mass Transfer*, Vol. 18, No. 7/8, 1975, pp. 901–910.

[10]Comini, G., Del-Guidice, S., Lewis, R. W., and Zienkiewicz, O. C., "Finite Element Solution of Non-linear Heat Conduction Problems with Special Reference to Phase Change," *International Journal for Numerical Methods in Engineering*, Vol. 8, No. 3, 1974, pp. 613–624.

[11]Shamsundar, N., and Sparrow, E. M., "Analysis of Multidimensional Conduction Phase Change via the Enthalpy Model," *Journal of Heat Transfer*, Vol. 97, No. 3, 1975, pp. 333–340.

[12]Chuang, Y. K., and Szekely, J., "On the Use of Green's Functions for Solving Melting or Solidification Problems," *International Journal of Heat and Mass Transfer*, Vol. 14, No. 9, 1971, pp. 1283–1295.

[13]Brebbia, C. A., *The Boundary Element Method for Engineers*, Penteel, London, England, 1978.

[14]Lynch, D. R., and Gray, W. G., "Finite Element Simulation of Flow in Deforming Regions," *Journal of Computational Physics*, Vol. 36, No. 2, 1980, pp. 135–153.

[15]Zhong, J., Chow, L. C., and Chang, W. S., "A Finite Eigenvalue Method for Solving Transient Heat Conduction Problems," AIAA Paper 90-0543, Jan. 1990.

[16]Garbow, B. S., Boyle, J. M., Dongarra, J. J., and Moler, C. B., *Matrix Eigensystem Routines—EISPACK Guide Extension*, Springer-Verlag, New York, 1977.